

Higgs-strahlung production process $e^+e^- \rightarrow Zh$ at the future Higgs factory in the Minimal Dilaton Model

Junjie Cao^{1,2}, Zhaoxia Heng¹, Dongwei Li¹, Liangliang Shang¹, Peiwen Wu³

¹ *Department of Physics, Henan Normal University, Xinxiang 453007, China*

² *Center for High Energy Physics, Peking University, Beijing 100871, China*

³ *State Key Laboratory of Theoretical Physics,*

Institute of Theoretical Physics, Academia Sinica, Beijing 100190, China

Abstract

We investigate the Higgs-strahlung production process $e^+e^- \rightarrow Zh$ at the future Higgs factory such as TLEP by including radiative corrections in the Minimal Dilaton Model (MDM), which extends the SM by one singlet scalar called dilaton. We consider various theoretical and experimental constraints on the model, and perform fits to the Higgs data taken from ATLAS, CMS and CDF+D0. Then for the 1σ surviving samples, we calculate the MDM predictions on the inclusive production rate $\sigma(e^+e^- \rightarrow Zh)$ at the 240-GeV Higgs factory, and also the signal rates of $e^+e^- \rightarrow Zh$ with the Higgs boson decaying to $b\bar{b}$ and $\gamma\gamma$. We have following observations: (1) In the heavy dilaton scenario, the deviation of $\sigma(e^+e^- \rightarrow Zh)$ from its SM prediction can vary from -15% to 85% , which mainly arises from the modification of the tree-level hZZ coupling and also the radiative correction induced by possibly large Higgs self-couplings. (2) The processes $e^+e^- \rightarrow Zh$ at the Higgs factory and $pp \rightarrow hh$ at 14-TeV LHC are complementary in limiting the MDM parameter space. Requiring the deviation of $\sigma(e^+e^- \rightarrow Zh)$ from its SM prediction to be less than 1% and that of $\sigma(pp \rightarrow hh)$ to be less than 50% , $\tan\theta_S$ in the MDM will be limited to be $-0.1 < \tan\theta_S < 0.3$, and the deviations of the signal rates are constrained to be $|R_{b\bar{b}}| < 2\%$ and $|R_{\gamma\gamma}| < 7\%$. Especially, the Higgs self-coupling normalized to its SM prediction is now upper bounded by about 4. (3) In the light dilaton scenario, the deviation of $\sigma(e^+e^- \rightarrow Zh)$ may reach -7% , and requiring its size to be less than 1% will result in $0 < \tan\theta_S < 0.1$, and $-10\% < R_{b\bar{b}}, R_{\gamma\gamma} < 1\%$.

PACS numbers: 12.60.Fr, 14.80.Cp

I. INTRODUCTION

In July 2012, the discovery of a new boson with mass around 125 GeV at the CERN Large Hadron Collider (LHC) [1, 2] marked a great triumph in the history of particle physics. With the growingly accumulated data, the properties of this newly discovered boson are in excellent agreement with those of the Higgs boson predicted by the Standard Model (SM), including the further measurements of its spin and parity quantum numbers [3, 4]. However, up to now, there is no evidence to establish whether the Higgs sector contains only one Higgs doublet. Instead, the Higgs-like resonance with mass about 125 GeV can also be well explained in many new physics models, such as low energy supersymmetric models [5, 6] and the dilaton models [7].

So far various Higgs couplings to SM fermions and vector bosons based on the current LHC data still have large uncertainties. Taking the hZZ coupling as an example, the measured value normalized to its SM prediction is $1.43 \pm 0.33(\text{stat}) \pm 0.17(\text{syst})$ for ATLAS result and 0.92 ± 0.28 for CMS result [8]. Nevertheless, at the future High Luminosity LHC (HL-LHC) with 300 fb^{-1} (3000 fb^{-1}) integrated luminosity, the precision of the C_{hZZ} measurement is expected to reach $4 - 6\%$ ($2 - 4\%$) [8]. Compared with the hadron collider, the future e^+e^- collider may have a stronger capability in the C_{hZZ} measurement through the Higgs-strahlung production $e^+e^- \rightarrow Zh$. For example, at the proposed International Linear Collider (ILC) with collision energy up to 1TeV and luminosity up to 1000 fb^{-1} , the precision may be improved to be near 0.5% [8]. And an even more remarkable precision of 0.05% may be achieved at the recently proposed Triple-Large Electron-Positron Collider (TLEP)[8], which is a new circular e^+e^- collider operated at $\sqrt{s} = 240 \text{ GeV}$ with 10^4 fb^{-1} integrated luminosity[9].

The story of the Higgs self-coupling, however, is quite different. By now such a coupling has basically not been constrained by the current Higgs data, while on the other hand, it can be quite large in some new physics models such as the Minimal Dilaton Model (MDM) [10–12]. Obviously, the next important task of experimentalists is to determine the coupling size as precise as possible, which is essential in reconstructing the Higgs potential and consequently determining the mechanism of the electro-weak symmetry breaking. At both the LHC and the ILC, the Higgs self-coupling can be measured directly through the Higgs pair production [13–15]. The recent studies suggest that a precision of 50% for the coupling

can be obtained through $pp \rightarrow hh \rightarrow bb\gamma\gamma$ at the HL-LHC with an integrated luminosity of 3000 fb^{-1} [8, 16], and it may be further improved to be around 13% at the ILC with collision energy up to 1TeV[8].

One interesting feature of the Higgs-strahlung production $e^+e^- \rightarrow Zh$ is that, while at tree level its rate is solely determined by the C_{hZZ} coupling, at loop level the rate also depends on the Higgs self-coupling and may be significantly altered by such a coupling. This brings us the possibility that apart from the direct Higgs pair production, the Higgs self-coupling may also be measured indirectly from the process $e^+e^- \rightarrow Zh$ with the e^+e^- collision energy below the di-Higgs threshold. As shown in [17], given that the inclusive cross section $\sigma(e^+e^- \rightarrow Zh)$ is measured with a precision of 0.4% at the TLEP[9], the Higgs self-coupling may be constrained to an accuracy of 28%.

In this work we take the MDM as an example to investigate the Higgs-strahlung production $e^+e^- \rightarrow Zh$ by including radiative corrections. We scan the MDM parameters by considering various experimental and theoretical constraints. Then for the surviving samples we calculate their predictions on $\sigma(e^+e^- \rightarrow Zh)$ at the 240-GeV TLEP, and investigate to what extent the parameters will be constrained given the future precision of the cross section measurement. Noting that more observables will be helpful to further limit the parameter space, we also perform a study on the signals of the Higgs-strahlung production with the Higgs boson decaying to $\gamma\gamma$ or $b\bar{b}$. We note that similar study has been done in supersymmetric models [18].

This work is organized as follows. In Sec. II, we briefly review the MDM and experimental and theoretical constraints on it. Then we calculate $\sigma(e^+e^- \rightarrow Zh)$ by including radiative corrections and discuss the capability of the Higgs factory to determine the model parameters in Sec. III. Finally, we summarize our conclusions in Sec. IV.

II. THE MINIMAL DILATON MODEL

The MDM is an extension of the SM by introducing a linearized singlet dilaton field S and a vector-like top partner T with the same quantum number as the right-handed top

quark. The low energy effective Lagrangian of the MDM is given by [10–12]

$$\begin{aligned} \mathcal{L} = & \mathcal{L}_{\text{SM}} - \frac{1}{2} \partial_\mu S \partial^\mu S - \frac{m_S^2}{2} S^2 - \frac{\lambda_S}{4!} S^4 - \frac{\kappa}{2} S^2 |H|^2 - m_H^2 |H|^2 - \frac{\lambda_H}{4} |H|^4 \\ & - \bar{T} \left(\not{D} + \frac{M}{f} S \right) T - [y' \bar{T}_R (q_{3L} \cdot H) + \text{h.c.}] , \end{aligned} \quad (1)$$

where \mathcal{L}_{SM} is the part of the SM Lagrangian without the Higgs potential, M represents the scale of a certain strong dynamics in which the fields T and S are involved, q_{3L} is the $SU(2)_L$ left-handed quark doublet of the third generation, and M_H , M_S , λ_S , κ and λ_H are all free parameters describing the new Higgs potential. The singlet dilaton field S and the doublet Higgs field H will mix with each other, which can be parameterized by the Higgs-dilaton mixing angle θ_S as

$$\begin{aligned} S &= f + h \sin \theta_S + s \cos \theta_S, \\ H &= \begin{pmatrix} \phi^+ \\ \frac{1}{\sqrt{2}}(v + h \cos \theta_S - s \sin \theta_S + i\phi^0) \end{pmatrix} \end{aligned} \quad (2)$$

with f and $v = 246$ GeV being the vacuum expectation values (vev) of S and H respectively, h and s denoting the mass eigenstates of the Higgs boson and the dialton, and ϕ^0 and ϕ^+ representing the Goldstone bosons. Similarly, q_{3L}^u and T will mix to form mass eigenstates t and t' so that

$$\begin{aligned} q_{3L}^u &= \cos \theta_L t_L + \sin \theta_L t'_L, \\ T_L &= -\sin \theta_L t_L + \cos \theta_L t'_L. \end{aligned} \quad (3)$$

If θ_S , f and physical masses m_h , m_s are taken as the input of the theory, one can re-express the dimensionless parameters λ_S , κ and λ_H as follows[12]

$$\begin{aligned} \lambda_S &= \frac{3|m_h^2 - m_s^2|}{2f^2} \left[\frac{m_h^2 + m_s^2}{|m_h^2 - m_s^2|} - \text{Sign}(\sin 2\theta_S) \cos 2\theta_S \right], \\ \kappa &= \frac{|m_h^2 - m_s^2|}{2fv} |\sin 2\theta_S|, \\ \lambda_H &= \frac{|m_h^2 - m_s^2|}{v^2} \left[\frac{m_h^2 + m_s^2}{|m_h^2 - m_s^2|} + \text{Sign}(\sin 2\theta_S) \cos 2\theta_S \right]. \end{aligned} \quad (4)$$

In this case, the trilinear interactions among h , s , ϕ^0 and ϕ^\pm are given by

$$C_{hhh} = v \left[\frac{3}{2} \lambda_H \cos^3 \theta_S + \lambda_S \eta^{-1} \sin^3 \theta_S + 3\kappa(\cos \theta_S \sin^2 \theta_S + \eta^{-1} \cos^2 \theta_S \sin \theta_S) \right], \quad (5)$$

$$C_{hss} = v \left[\kappa(\cos^3 \theta_S + \eta^{-1} \sin^3 \theta_S) + \left(\frac{3}{2} \lambda_H - 2\kappa\right) \cos \theta_S \sin^2 \theta_S + \eta^{-1}(\lambda_S - 2\kappa) \cos^2 \theta_S \sin \theta_S \right], \quad (6)$$

$$C_{hhs} = v \left[\kappa(-\sin^3 \theta_S + \eta^{-1} \cos^3 \theta_S) - \left(\frac{3}{2} \lambda_H - 2\kappa\right) \sin \theta_S \cos^2 \theta_S + \eta^{-1}(\lambda_S - 2\kappa) \sin^2 \theta_S \cos \theta_S \right], \quad (7)$$

$$C_{h\phi^0\phi^0} = v \left(\kappa \eta^{-1} \sin \theta_S + \frac{\lambda_H}{2} \cos \theta_S \right), \quad (8)$$

$$C_{h\phi^+\phi^-} = v \left(\kappa \eta^{-1} \sin \theta_S + \frac{\lambda_H}{2} \cos \theta_S \right) \quad (9)$$

with $\eta \equiv \frac{v}{f}$, and the normalized couplings of h and s with Z or ϕ^0 are given by

$$\begin{aligned} C_{hZZ}/SM &= C_{hZ\phi^0}/SM = \cos \theta_S, & C_{sZZ}/SM &= C_{sZ\phi^0}/SM = -\sin \theta_S, \\ C_{hhZZ}/SM &= \cos^2 \theta_S, & C_{hsZZ}/SM &= -\cos \theta_S \sin \theta_S, & C_{ssZZ}/SM &= \sin^2 \theta_S. \end{aligned} \quad (10)$$

In the following we differentiate two scenarios according to the dilaton mass[12]:

- Heavy dilaton scenario: $m_s > m_h$. An important feature of this scenario is that the trilinear Higgs self-coupling C_{hhh} may be very large.
- Light dilaton scenario: $m_s < \frac{m_h}{2} \simeq 62$ GeV. In this scenario, the Higgs exotic decay $h \rightarrow ss$ is open with a possible large branching ratio, while C_{hhh}/SM is around at either 1 or 0.

For each parameter point of these scenarios, we impose the constraints similar to what we did in [12], which are given by

- (1) Vacuum stability of the scalar potential and absence of the Landau pole up to 1TeV.
- (2) Bounds from the search for Higgs-like scalar at LEP, Tevatron and LHC.
- (3) $m_{t'} \geq 1\text{TeV}$ as suggested by the LHC search for top quark partner[19] and constraints from the precision electroweak data[10]. With this constraint, we have $\cos \theta_L > 0.97$ and consequently $C_{htt}/SM \simeq \cos \theta_S$ [12].

- (4) Constraints from the measured Higgs properties. In implementing this constraint, we use the combined data (22 sets) from ATLAS, CMS and CDF+D0 and perform a fit with the same method as that in [20–22]. We obtained $\chi^2_{min} = 18.66$ in the MDM, which is less than χ^2 for the SM ($\chi^2_{SM} = 18.79$), and paid particular attention to 1σ samples in the fit.

As shown in [12], parameter points satisfying the above constraints will predict $\cos\theta_S > 0.92$, and $C_{h\bar{t}t'}/C_{h\bar{t}t}^{SM} < 0.1$. As will be seen below, this feature is beneficial for our analysis.

III. CALCULATIONS AND NUMERICAL RESULTS

In the SM, the radiative corrections to the Higgs-strahlung production process $e^+e^- \rightarrow Zh$ come from the Z boson self-energy, the vertex corrections to Ze^+e^- , he^+e^- , ZZh and $Z\gamma h$ interactions, and also box contributions[23, 24]. The full calculation of these corrections is quite complex (e.g. more than sixty diagrams need to be calculated) and it was shown recently that the total weak correction is 5% for $m_h = 125\text{GeV}$ and $\sqrt{s} = 240\text{GeV}$ [25]. About the corresponding corrections in the MDM, we have following observations

- Although the contribution induced by the Higgs self-coupling is only 2% in the SM[25], it is potentially large in the MDM since the self-couplings among the scalars may be greatly enhanced[12]. In this work, we will focus on such a contribution.
- The correction mediated by t' quark can be safely neglected since t' is heavy and meanwhile $C_{h\bar{t}t'}$ is relatively small.
- For loops that involves the sZZ interaction and meanwhile do not involve possible large self-couplings among the scalars, their contributions are negligible since the dilaton is highly singlet dominated.
- For the rest contributions, they can be obtained from the corresponding SM results in [23] by scaling with a factor of either $\cos^3\theta_S$ or $\cos\theta_S$. We find by detailed calculation that the size of the former contribution, i.e. that obtained by the scaling factor of $\cos^3\theta_S$, is -0.4% in the SM, and the latter contribution is 3.4% .

Based on these observations, we conclude that the deviation of the inclusive production rate $\sigma(e^+e^- \rightarrow Zh)$ from its SM prediction, which is generally called genuine new physics

contribution, is given by

$$\begin{aligned}
R &\equiv \frac{\sigma_{\text{MDM}}^{\text{LOOP}}(e^+e^- \rightarrow Zh) - \sigma_{\text{SM}}^{\text{LOOP}}(e^+e^- \rightarrow Zh)}{\sigma_{\text{SM}}^0(e^+e^- \rightarrow Zh)} \\
&\simeq \cos^2 \theta_S + 0.034 \cos^2 \theta_S - 0.004 \cos^4 \theta_S + \frac{\delta\sigma_{\text{MDM}}^{\text{scalar}}(e^+e^- \rightarrow Zh)}{\sigma_{\text{SM}}^0(e^+e^- \rightarrow Zh)} - 1.05 \\
&\simeq 1.03 \cos^2 \theta_S + \frac{\delta\sigma_{\text{MDM}}^{\text{scalar}}(e^+e^- \rightarrow Zh)}{\sigma_{\text{SM}}^0(e^+e^- \rightarrow Zh)} + 0.001 \sin^2 2\theta_S - 1.05
\end{aligned} \tag{11}$$

where $\sigma_{\text{MDM}}^{\text{LOOP}}$ and $\sigma_{\text{SM}}^{\text{LOOP}}$ are the cross sections at one loop level in the MDM and the SM respectively, σ_{SM}^0 is the SM prediction on the cross section at tree level, and $\delta\sigma_{\text{MDM}}^{\text{scalar}}$ denotes the correction induced by the self-couplings among the scalars with the corresponding diagrams given in Fig.1. Note that the first term on the right hand of the second equation corresponds to the tree-level contribution, which differs from its SM prediction due to the modified hZZ coupling by a factor $\cos \theta_S$. Also note that the constraints have required $\cos \theta_S > 0.92$, so the deviation R mainly arises from the modification of the tree-level hZZ coupling and $\delta\sigma_{\text{MDM}}^{\text{scalar}}$.

In this work, we take $m_Z = 91.19\text{GeV}$, $\alpha = 1/128$ [26] and $m_h = 125\text{GeV}$, and fix the e^+e^- collision energy at 240 GeV. We obtained $\sigma_{\text{SM}}^0(e^+e^- \rightarrow Zh) = 236\text{fb}$, which is in accordance with the result in [9]. In our calculations of $\delta\sigma_{\text{MDM}}^{\text{scalar}}$, we adopt the Feynman-'t Hooft gauge, and therefore the diagram involving the Goldstone fields must be considered. Moreover, we note from Fig.1 that, except for the dilaton mass, the masses of the particles in the loops are fixed, and meanwhile, since the dilaton coupling with Z boson is very small due to its singlet-dominated nature, its induced contribution should be relatively small if C_{hss} or C_{hhs} is not much larger than C_{hhh} . These features imply that $\delta\sigma_{\text{MDM}}^{\text{scalar}}$ or R can be expressed in a semi-analytic way, which is given by

$$\begin{aligned}
R &\simeq 1.03 \cos^2 \theta_S + 0.02 \times \cos \theta_S \times \frac{C_{hhh}}{\text{SM}} + 0.000146 \times \left(\frac{C_{hhh}}{\text{SM}}\right)^2 \\
&\quad + 0.001 \sin^2 2\theta_S - 1.05.
\end{aligned} \tag{12}$$

In above equation, the second term on the right side reflects the interference between the tree-level contribution and the correction from the self-couplings, the third represents the pure self-coupling contribution which can not be neglected if $C_{hhh}/\text{SM} \gg 1$, and the fourth term can be safely neglected given $\cos \theta_S > 0.92$. For the results presented below, we obtain the value of $\delta\sigma_{\text{MDM}}^{\text{scalar}}$ by exact calculation, and we checked that for nearly all the surviving samples, Eq.(12) is a good approximation.

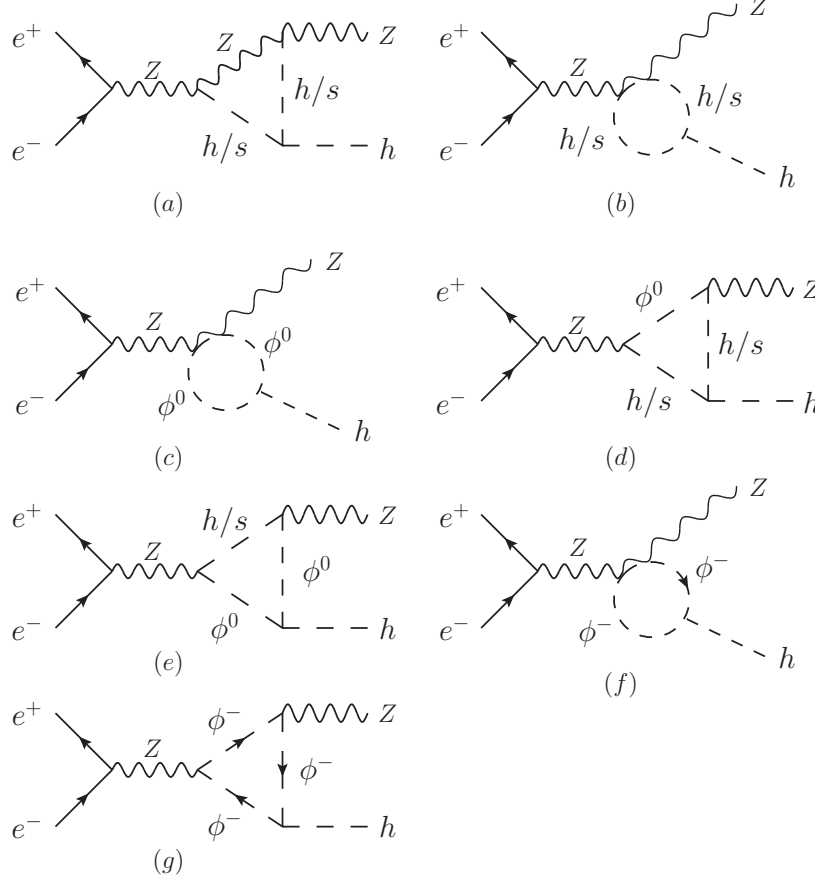


FIG. 1: Feynman diagrams for the Higgs-strahlung production $e^+e^- \rightarrow Zh$ in the MDM with corrections from the Higgs self-couplings at NLO in the Feynman-'t Hooft gauge.

A. Numerical results in the heavy dilaton scenario

For the heavy dilaton scenario, we consider the constraints listed in Sect. II and scan the relevant parameters in the following ranges like what we did in [12]

$$1 \leq \eta^{-1} < 10, \quad 130 \text{ GeV} < m_s < 1 \text{ TeV}, \quad |\tan \theta_S| < 2, \quad 1 \text{ TeV} < m_{t'} < 3 \text{ TeV}. \quad (13)$$

Then we investigate the properties of the 1σ samples, which satisfy $\chi^2 - \chi_{min}^2 \leq 2.3$.

In Fig.2 we project the 1σ samples on the plane of C_{hhh}/SM versus $\cos \theta_S$ and also show some lines corresponding to specific values of R calculated from Eq.(12). One can learn the following features:

- Due to the small coefficients of the second and third terms in Eq.(12), a given value of R in Eq.(12) corresponds to a very prolate ellipse on the whole plane of C_{hhh}/SM versus $\cos \theta_S$ after neglecting the term proportional to $\sin^2 2\theta_S$. For $\cos \theta_S > 0.92$, the

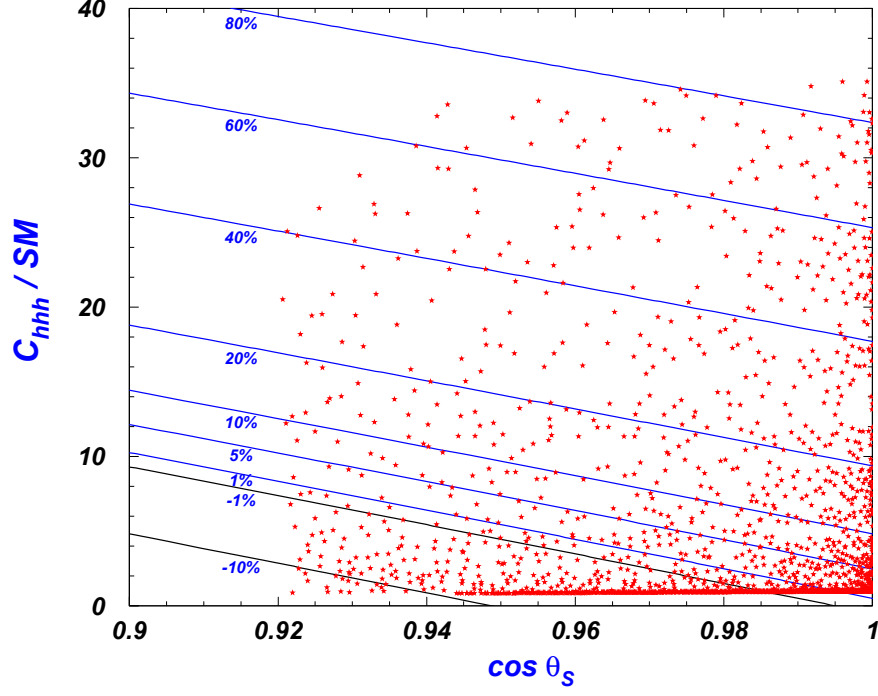


FIG. 2: The scatter plot of the 1σ samples in the heavy dilaton scenario, projected on the plane of C_{hhh}/SM versus $\cos \theta_S$. The lines denote various specific values of the deviation R calculated from Eq.(12).

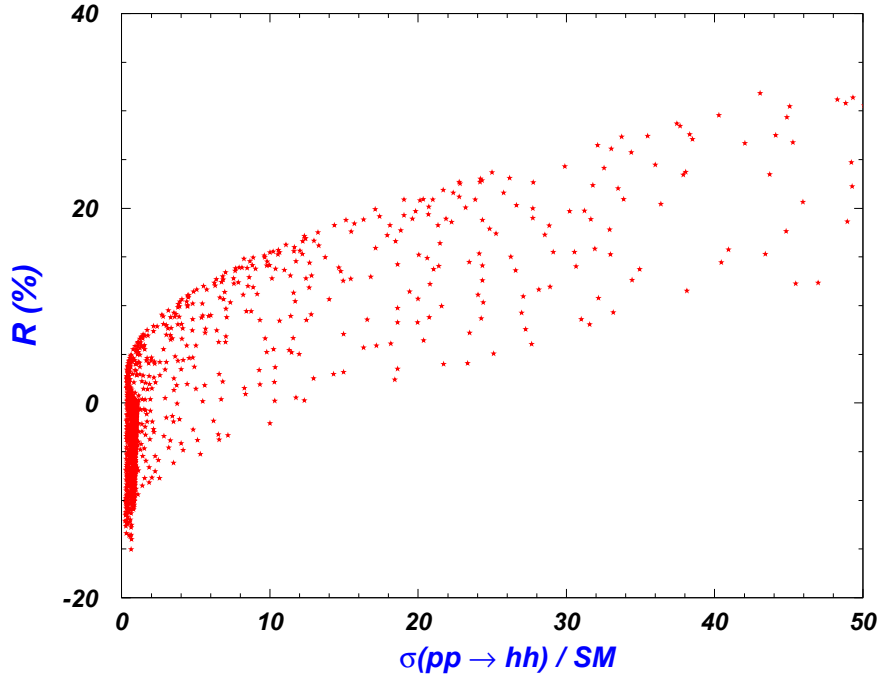


FIG. 3: Same as Fig.2, but projected on the plane of R versus the normalized cross section rate $\sigma(pp \rightarrow hh)/SM$ at the 14-TeV LHC.

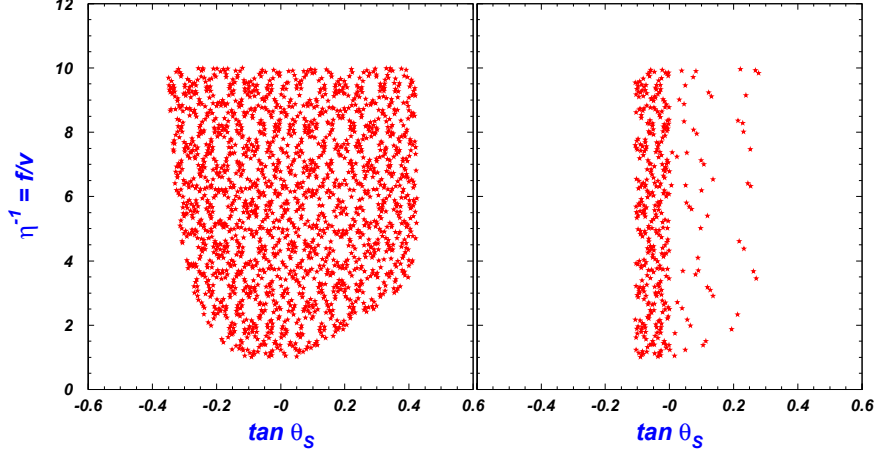


FIG. 4: Same as Fig.2, but projected on the plane of $\eta^{-1} = f/v$ versus $\tan \theta_S$. The left panel shows all the 1σ samples, while samples in the right panel are further required to satisfy $|R| < 1.0\%$ and $|\sigma(pp \rightarrow hh)/SM - 1| < 50\%$.

ellipse curves turn out to be nearly straight lines in Fig.2.

- As indicated by Eq.(12), the tree-level modification of the hZZ coupling is to decrease the inclusive rate, while the effect of the correction induced by the self-couplings is to increase the rate. For the 1σ samples considered, the deviation R varies from -15% to 85% . Such possible large deviation is due to a large uncertainty in determining the hZZ coupling from current Higgs data as well as currently a very weak constraint on the self-couplings.

Obviously, if R is moderately large, two loop or higher order corrections should also be taken into account.

With the upgraded energy and luminosity of the LHC, C_{hhh} may be measured directly through the Higgs pair production since it affects the production rate through the parton process $gg \rightarrow h^* \rightarrow hh$. As shown in Fig.6 of [12], for $C_{hhh}/SM \gtrsim 2.5$ in the heavy dilaton scenario of the MDM, the normalized cross section $\sigma(pp \rightarrow hh)/SM$ at the 14-TeV LHC increases monotonically as C_{hhh}/SM becomes larger. In order to compare the effect of the Higgs self-coupling at the LHC with that at the future Higgs factory, we show the correlation of $\sigma(pp \rightarrow hh)$ at the 14-TeV LHC with $\sigma(e^+e^- \rightarrow Zh)$ at 240-GeV TLEP in Fig.3. This figure manifests that a $\sigma(pp \rightarrow hh)/SM$ of several tens usually corresponds to a R larger than 5%. For example, in the case of $\sigma(pp \rightarrow hh)/SM = 40$, R varies from 10% to 30%. While on the other hand, even for $\sigma(pp \rightarrow hh)/SM \sim 1$, the size of R may still

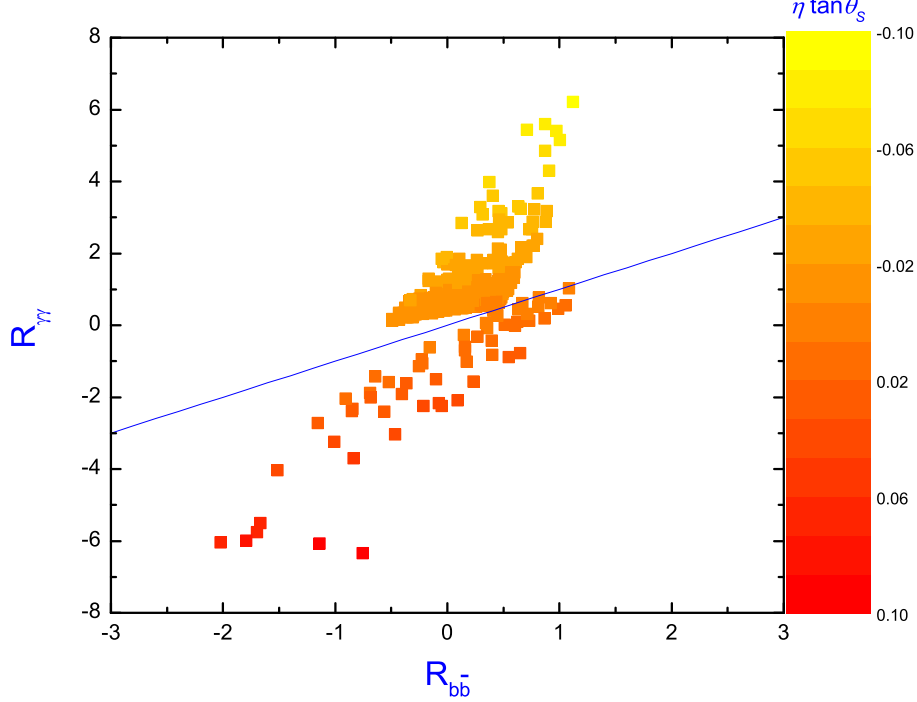


FIG. 5: Samples in the right panel of Fig.4, but projected on the plane of $R_{\gamma\gamma}$ versus $R_{b\bar{b}}$, where dependence on $\eta \tan \theta_S$ is also shown. For clarity, we draw a blue line corresponding to $R_{b\bar{b}} = R_{rr}$.

be moderately large, changing from -15% to 5% . These features tell us that the processes $pp \rightarrow hh$ and $e^+e^- \rightarrow Zh$ are complementary in limiting the parameters of the MDM.

In order to investigate the capability of the future experiments to detect the parameter space of the MDM, we assume a measurement precision of 1.0% for $\sigma(e^+e^- \rightarrow Zh)$ at 240 GeV [9] and 50% for $\sigma(pp \rightarrow hh)$ at 14 TeV[8, 16]. Then we show the allowed parameter region on $\eta^{-1} - \tan \theta_S$ plane in the right panel of Fig.4 by requiring the 1σ samples to further satisfy $|R| < 1.0\%$ and $|\sigma(pp \rightarrow hh)/SM - 1| < 50\%$. For comparison, we also show the 1σ samples in the left panel of Fig.4 without the requirement. Fig.4 indicates that $\tan \theta_S$ is allowed to be within $-0.4 < \tan \theta_S < 0.4$ and $-0.1 < \tan \theta_S < 0.3$ before and after the requirement respectively. Furthermore, we checked that, after imposing the requirement, the number of the 1σ samples in our random scan is reduced by more than 80% , and now C_{hhh} satisfies $0.98 \leq C_{hhh}/SM \leq 4.4$. This reflects the great power of the future experiments in limiting the MDM.

Since the MDM parameters can still survive in a fairly wide region after considering the measurement of the inclusive production rate at future Higgs factory, we need to consider more observables to limit the model. So we also investigate the signal rates of $e^+e^- \rightarrow$

$Zh \rightarrow Zb\bar{b}, Z\gamma\gamma$. Similar to R , we define the deviations of the signal rates from their SM predictions by

$$\begin{aligned} R_{b\bar{b}} &\equiv \frac{\sigma_{\text{MDM}}^{\text{LOOP}}(e^+e^- \rightarrow Zh)Br_{\text{MDM}}(h \rightarrow b\bar{b}) - \sigma_{\text{SM}}^{\text{LOOP}}(e^+e^- \rightarrow Zh)Br_{\text{SM}}(h \rightarrow b\bar{b})}{\sigma_{\text{SM}}^0(e^+e^- \rightarrow Zh)Br_{\text{SM}}(h \rightarrow b\bar{b})}, \\ R_{\gamma\gamma} &\equiv \frac{\sigma_{\text{MDM}}^{\text{LOOP}}(e^+e^- \rightarrow Zh)Br_{\text{MDM}}(h \rightarrow \gamma\gamma) - \sigma_{\text{SM}}^{\text{LOOP}}(e^+e^- \rightarrow Zh)Br_{\text{SM}}(h \rightarrow \gamma\gamma)}{\sigma_{\text{SM}}^0(e^+e^- \rightarrow Zh)Br_{\text{SM}}(h \rightarrow \gamma\gamma)} \quad (14) \end{aligned}$$

where $Br_{\text{MDM}}(h \rightarrow b\bar{b})$ and $Br_{\text{SM}}(h \rightarrow b\bar{b})$ denote the branching ratio of $h \rightarrow b\bar{b}$ in the MDM and the SM respectively, and similar notation is applied for $h \rightarrow \gamma\gamma$. In the heavy dilaton scenario, $R_{b\bar{b}}$ and $R_{\gamma\gamma}$ can be approximated by[12]

$$R_{b\bar{b}} \simeq (R + 1.05) \cdot \frac{\cos^2 \theta_S \Gamma_{SM}^{b\bar{b}} \Gamma_{SM}}{\cos^2 \theta_S \Gamma_{SM} \Gamma_{SM}^{b\bar{b}}} - 1.05 \simeq R, \quad (15)$$

$$R_{\gamma\gamma} \simeq (R + 1.05) \cdot (1 - 0.27\eta \tan \theta_S)^2 - 1.05 \quad (16)$$

where Γ_{SM} and $\Gamma_{SM}^{b\bar{b}}$ denote respectively the total width of the Higgs boson and the partial width of $h \rightarrow b\bar{b}$ in the SM. Note that the above approximations are good only for a sufficiently large R , but anyhow, they are helpful to understand our results. In Fig.5, we project the samples in the right panel of Fig.4 on the plane of $R_{\gamma\gamma}$ versus $R_{b\bar{b}}$ for different values of $\eta \tan \theta_S$. This figure indicates that $R_{b\bar{b}}$ is basically constrained in the range of $|R_{b\bar{b}}| < 2\%$, while $|R_{\gamma\gamma}|$ can maximally reach 7%. Considering that the expected precisions of measured $\sigma \cdot BR(h \rightarrow b\bar{b})$ and $\sigma \cdot BR(h \rightarrow \gamma\gamma)$ at 240-GeV TLEP can reach the level of 0.2% and 3.0% respectively [8], one can expect that by the measurement of the $b\bar{b}$ and $\gamma\gamma$ signal rates, one can get additional information about $\eta \tan \theta_S$ if the MDM is a correct theory.

B. Numerical results in the light dilaton scenario

In the light dilaton scenario we scan following parameter ranges by considering the constraints listed in Sec. II

$$1 \leq \eta^{-1} < 10, \quad 0 \text{ GeV} < m_s < 62 \text{ GeV}, \quad |\tan \theta_S| < 2, \quad 1\text{TeV} < m_{t'} < 3\text{TeV}, \quad (17)$$

and investigate the properties of the 1σ samples, which are now defined by $\chi^2 - \chi_{\min}^2 \leq 1.0$ [12]. Compared with the heavy dilaton scenario, the light dilaton scenario has two distinct features. One is the Higgs exotic decay $h \rightarrow ss$ is open with a possible large branching ratio.

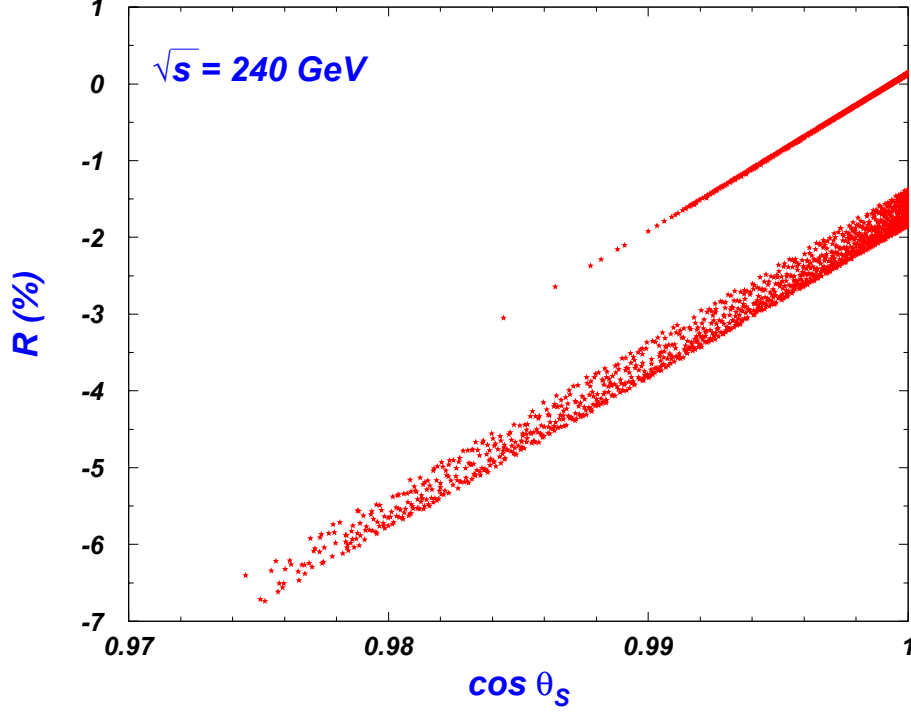


FIG. 6: The scatter plot of the 1σ samples in the light dilaton scenario, projected on the plane of the deviation R versus $\cos \theta_S$.

So this scenario is more tightly constrained by current Higgs data. And the other is the Higgs self-coupling strength C_{hhh}/SM is relatively small, around at either 1 or 0. As a result, the deviation R mainly comes from the modified hZZ coupling, so $R \simeq \cos^2 \theta_S - 1$. In Fig.6 we project the 1σ samples on the plane of deviation R versus $\cos \theta_S$. As expected, the size of the deviation R monotonically decreases as $\cos \theta_S$ approach 1, and it can maximally reach 7%. This figure also shows that there are two separated regions of R . We checked that it is due to the discontinuousness of C_{hhh}/SM , that is, the upper region corresponds to $C_{hhh}/SM \simeq 1$, while the lower region corresponds to $C_{hhh}/SM \simeq 0$.

Adopting the same analysis as Fig.4, we show the 1σ samples projected on the plane of $\eta^{-1} = f/v$ versus $\tan \theta_S$ in Fig.7, where the left panel shows all 1σ samples, while for comparison the right panel shows samples that further satisfy the requirement $|R| < 1.0\%$. Here we do not consider the deviation of $\sigma(pp \rightarrow hh)$ because it is very small in the light dilation scenario [12]. Fig.7 clearly shows that the MDM parameter space in the light dilaton scenario is also strongly constrained resulting in $0 < \tan \theta_S < 0.1$, in contrast with $-0.24 < \tan \theta_S < 0.2$ without the requirement of $|R| < 0.1$. Moreover, we checked that after the requirement, the number of the 1σ samples in the left panel of Fig.7 is reduced by more

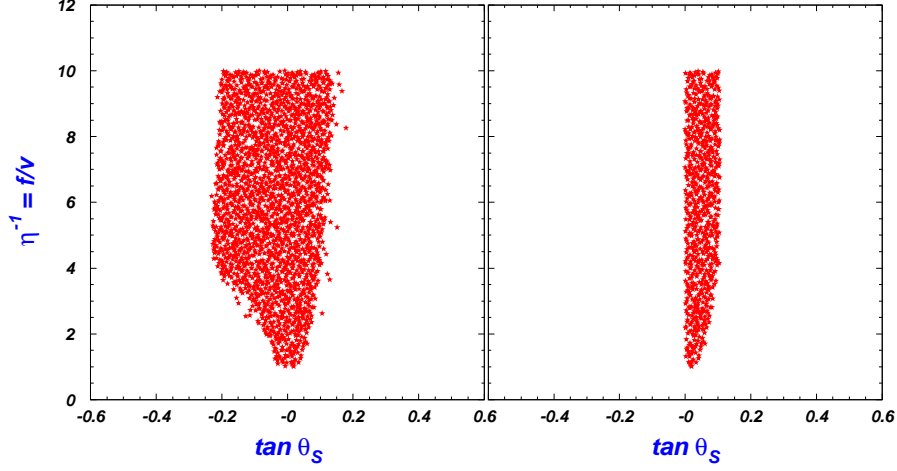


FIG. 7: Scatter plot of the 1σ samples in the light dilaton scenario, projected on the plane of $\eta^{-1} = f/v$ versus $\tan \theta_S$. The left panel shows all 1σ samples, while the right panel shows samples further satisfying $|R| < 1.0\%$.

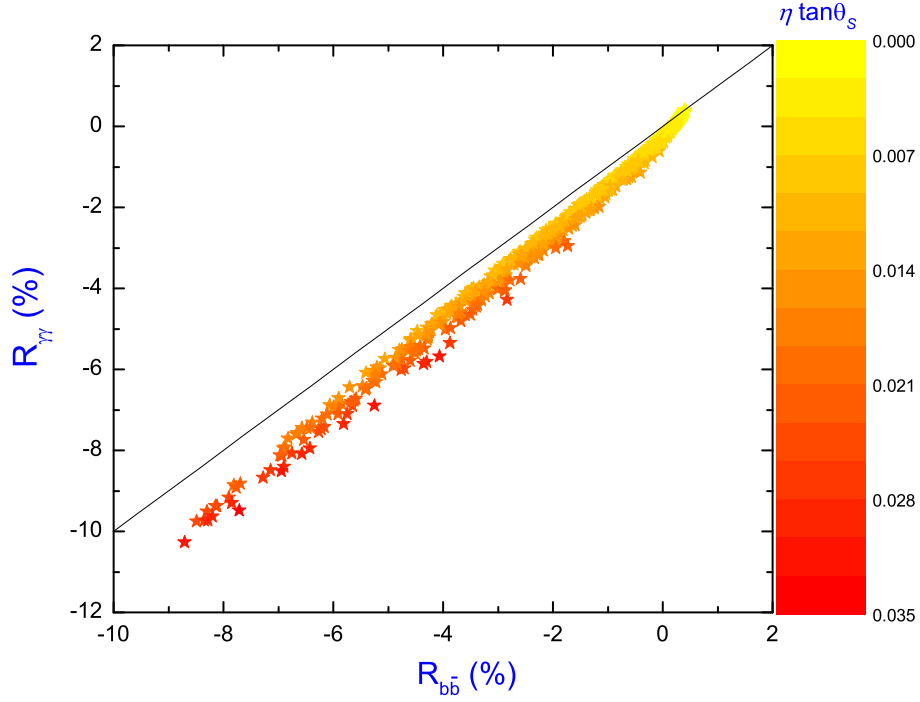


FIG. 8: Same as Fig.6, but projected on the plane of $R_{\gamma\gamma}$ versus $R_{b\bar{b}}$, and also shows the dependence on $\eta \tan \theta_S$.

than 70%.

Similar to what we did in the heavy dilaton scenario, we also investigate the signal

deviations $R_{b\bar{b}}$ and $R_{\gamma\gamma}$, which can now be expressed as

$$\begin{aligned} R_{b\bar{b}} &\simeq (R + 1.05) \frac{\cos^2 \theta_S \Gamma_{SM}^{b\bar{b}}}{\cos^2 \theta_S \Gamma_{SM} + \Gamma_{ss} \Gamma_{SM}^{b\bar{b}}} - 1.05 \\ &\simeq (R + 1.05)(1 - Br(h \rightarrow ss)) - 1.05 \end{aligned} \quad (18)$$

$$R_{\gamma\gamma} \simeq (R + 1.05)(1 - 0.27\eta \tan \theta_S)^2(1 - Br(h \rightarrow ss)) - 1.05, \quad (19)$$

where Γ_{ss} is the width of $h \rightarrow ss$ in the MDM. In Fig.8 we show the relationship between $R_{\gamma\gamma}$ and $R_{b\bar{b}}$, and their dependence on $\eta \tan \theta_S$. From this figure we can see that $R_{\gamma\gamma}$ and $R_{b\bar{b}}$ follow a nearly linear correlation since now $\eta \tan \theta_S$ is very small, i.e. $|\eta \tan \theta_S| < 0.035$. One can also see that even with the requirement $|R| < 1\%$, $R_{b\bar{b}}$ and $R_{\gamma\gamma}$ may reach -10% . This is because the branching ratio of $h \rightarrow ss$ may still be moderate large under the constraint of current Higgs data. Note that generally $|R_{\gamma\gamma}|$ is slightly larger than $|R_{b\bar{b}}|$, which can be understood by the positiveness of $\tan \theta_S$ in Eq.(19).

IV. SUMMARY AND CONCLUSION

In this work, we intend to investigate the capability of the future Higgs factory such as TLEP in detecting the parameter space of the MDM, which extends the SM by one singlet scalar called dilaton. For this end, we calculate the Higgs-strahlung production process $e^+e^- \rightarrow Zh$ at the future Higgs factory by including radiative corrections in the model. We consider various theoretical and experimental constraints on the model, such as the vacuum stability, absence of Landau pole, the electro-weak precision data and the LHC search for Higgs boson, and perform fits to the Higgs data taken from ATLAS, CMS and CDF+D0. Then for the 1σ surviving samples, we investigate the MDM predictions on the inclusive production rate $\sigma(e^+e^- \rightarrow Zh)$ at the 240-GeV Higgs factory, and also the signal rates of $e^+e^- \rightarrow Zh$ with the Higgs boson decaying to $b\bar{b}$ and $\gamma\gamma$. We have following observations: (1) In the heavy dilaton scenario, the deviation of $\sigma(e^+e^- \rightarrow Zh)$ from its SM prediction can vary from -15% to 85% , which mainly arises from the modification of the tree-level hZZ coupling and also the radiative correction induced by possibly large Higgs self-couplings. (2) The processes $e^+e^- \rightarrow Zh$ at the Higgs factory and $pp \rightarrow hh$ at 14-TeV LHC are complementary in limiting the MDM parameter space. Requiring the deviation of $\sigma(e^+e^- \rightarrow Zh)$ from its SM prediction to be less than 1% and that of $\sigma(pp \rightarrow hh)$ to be less than 50% , $\tan \theta_S$ in the MDM will be limited to be $-0.1 < \tan \theta_S < 0.3$, the deviations

of the signal rates are constrained to be $|R_{b\bar{b}}| < 2\%$ and $|R_{\gamma\gamma}| < 7\%$, and the Higgs self-coupling normalized to its SM prediction is upper bounded by about 4. (3) In the light dilaton scenario, the deviation of $\sigma(e^+e^- \rightarrow Zh)$ may reach -7% , and requiring its size to be less than 1% will result in $0 < \tan\theta_S < 0.1$, and $-10\% < R_{b\bar{b}}, R_{\gamma\gamma} < 1\%$.

Acknowledgement

We thank Cheng Li, Jing-Ya Zhu and Li Lin Yang for helpful discussion at the early stage of this work. This work is supported by the National Natural Science Foundation of China (NNSFC) under grant No. 10775039, 11075045, 11275245, 10821504 and 11305050, by Program for New Century Excellent Talents in University, by the Project of Knowledge Innovation Program (PKIP) of Chinese Academy of Sciences under grant No. KJCX2.YW.W10, and by Specialized Research Fund for the Doctoral Program of Higher Education with grant No. 20124104120001.

-
- [1] G. Aad *et al.* [ATLAS Collaboration], Phys. Lett. B **716** (2012) 1 [arXiv:1207.7214 [hep-ex]].
 - [2] S. Chatrchyan *et al.* [CMS Collaboration], Phys. Lett. B **716** (2012) 30 [arXiv:1207.7235 [hep-ex]].
 - [3] The ATLAS Collaboration, ATLAS-CONF-2013-040; Phys. Lett. B **726**, 120 (2013) [arXiv:1307.1432 [hep-ex]].
 - [4] S. Chatrchyan *et al.* [CMS Collaboration], Phys. Rev. Lett. **110**, 081803 (2013) [arXiv:1212.6639 [hep-ex]].
 - [5] M. Carena *et al.*, JHEP **1203**, 014 (2012); S. Heinemeyer, O. Stal and G. Weiglein, Phys. Lett. B **710**, 201 (2012); J. Cao *et al.*, Phys. Lett. B **710**, 665 (2012); N. D. Christensen, T. Han, S. Su, Phys. Rev. D **85** (2012) 115018; K. Hagiwara, J. S. Lee, J. Nakamura, JHEP **1210** (2012) 002; P. Bechtle *et al.*, Eur. Phys. J. C **73** (2013) 2354;
 - [6] U. Ellwanger, JHEP **1203**, 044 (2012); J. Cao *et al.*, JHEP **1203**, 086 (2012); U. Ellwanger, C. Hugonie, Adv. High Energy Phys. **2012** (2012) 625389; J. Cao *et al.*, JHEP **1210**, 079 (2012); J. F. Gunion, Y. Jiang, S. Kraml, Phys. Lett. B **710** (2012) 454; JHEP **1210** (2012) 072; S. F. King *et al.*, Nucl. Phys. B **860** (2012) 207; Nucl. Phys. B **870** (2013) 323; K. Agashe,

- Y. Cui and R. Franceschini, JHEP **1302** (2013) 031; K. Kowalska *et al.*, Phys. Rev. D **87** (2013) 115010; T. Gherghetta *et al.*, JHEP **1302** (2013) 032; N. D. Christensen, T. Han, Z. Liu and S. Su, JHEP **1308** (2013) 019; M. Badziak *et al.*, JHEP **1306** (2013) 043; S. Moretti, S. Munir and P. Poulose, Phys. Rev. D **89**, 015022 (2014); S. Munir, *et al.*, Phys. Rev. D **88**, 055017 (2013); S. Munir, Phys. Rev. D **89**, 095013 (2014).
- [7] B. Bellazzini, *et al.*, Eur. Phys. J. C **73**, 2333 (2013) [arXiv:1209.3299 [hep-ph]]; Z. Chacko, R. Franceschini and R. K. Mishra, JHEP **1304**, 015 (2013) [arXiv:1209.3259 [hep-ph]]; D. Elander and M. Piai, Nucl. Phys. B **867**, 779 (2013) [arXiv:1208.0546 [hep-ph]]; S. Matsuzaki and K. Yamawaki, Phys. Lett. B **719**, 378 (2013) [arXiv:1207.5911 [hep-ph]]; Phys. Rev. D **86**, 115004 (2012) [arXiv:1209.2017 [hep-ph]]; Phys. Rev. D **86**, 035025 (2012) [arXiv:1206.6703 [hep-ph]]; Phys. Rev. D **85**, 095020 (2012) [arXiv:1201.4722 [hep-ph]]; D. - W. Jung and P. Ko, Phys. Lett. B **732**, 364 (2014).
- [8] S. Dawson, A. Gribsan, H. Logan, *et al.*, arXiv:1310.8361 [hep-ex]; T. Han, Z. Liu and J. Sayre, arXiv:1311.7155 [hep-ph]; M. E. Peskin, arXiv:1312.4974 [hep-ph]; P. Bechtle, *et al.*, arXiv:1403.1582 [hep-ph];
- [9] M. Koratzinos, *et al.*, arXiv:1305.6498 [physics.acc-ph]; M. Bicer *et al.* [TLEP Design Study Working Group Collaboration], JHEP **1401**, 164 (2014) [arXiv:1308.6176 [hep-ex]].
- [10] T. Abe *et al.*, Phys. Rev. D **86** (2012) 115016.
- [11] T. Abe *et al.*, EPJ Web Conf. **49** (2013) 15018, [arXiv:1303.0935 [hep-ph]].
- [12] J. Cao, *et al.*, JHEP **1401**, 150 (2014) [arXiv:1311.6661 [hep-ph]].
- [13] J. Baglio, *et al.*, JHEP **1304**, 151 (2013) [arXiv:1212.5581 [hep-ph]]; D. Y. Shao, C. S. Li, H. T. Li and J. Wang, JHEP **1307**, 169 (2013) [arXiv:1301.1245 [hep-ph]]; D. de Florian and J. Mazzitelli, Phys. Lett. B **724**, 306 (2013) [arXiv:1305.5206 [hep-ph]]; Phys. Rev. Lett. **111**, 201801 (2013) [arXiv:1309.6594 [hep-ph]]; L. Liu-Sheng, *et al.*, Phys. Rev. D **89**, 073001 (2014) [arXiv:1401.7754 [hep-ph]].
- [14] For SUSY prediction on Higgs pair production, see for example, J. Cao, *et al.*, JHEP **1304**, 134 (2013) [arXiv:1301.6437 [hep-ph]]; Z. Heng, L. Shang and P. Wan, JHEP **1310**, 047 (2013) [arXiv:1306.0279 [hep-ph]]; D. T. Nhung, M. Muhlleitner, J. Streicher and K. Walz, JHEP **1311**, 181 (2013) [arXiv:1306.3926 [hep-ph]]; U. Ellwanger, JHEP **1308**, 077 (2013) [arXiv:1306.5541 [hep-ph]]; C. Han, X. Ji, L. Wu, P. Wu and J. M. Yang, JHEP **1404**, 003 (2014) [arXiv:1307.3790 [hep-ph]].

- [15] For Higgs pair production in new physics models other than SUSY, see for example, J. Liu, X. -P. Wang and S. -h. Zhu, arXiv:1310.3634 [hep-ph]; N. Haba, K. Kaneta, Y. Mimura and E. Tsedenbaljir, Phys. Rev. D **89**, 015018 (2014) [arXiv:1311.0067 [hep-ph]]; Q. Li, Q. -S. Yan and X. Zhao, Phys. Rev. D **89**, 033015 (2014) [arXiv:1312.3830 [hep-ph]]; Z. Heng, L. Shang, Y. Zhang and J. Zhu, JHEP **1402**, 083 (2014) [arXiv:1312.4260 [hep-ph]]. L. Wei-Hua, *et al.* arXiv:1403.2782 [hep-ph];
- [16] F. Goertz, A. Papaefstathiou, L. L. Yang and J. Zurita, JHEP **1306**, 016 (2013) [arXiv:1301.3492 [hep-ph]]; R. S. Gupta, H. Rzehak and J. D. Wells, Phys. Rev. D **88**, 055024 (2013) [arXiv:1305.6397 [hep-ph]]; A. J. Barr, M. J. Dolan, C. Englert and M. Spannowsky, Phys. Lett. B **728**, 308 (2014) [arXiv:1309.6318 [hep-ph]]; V. Barger, L. L. Everett, C. B. Jackson and G. Shaughnessy, Phys. Lett. B **728**, 433 (2014) [arXiv:1311.2931 [hep-ph]]; D. E. F. de Lima, A. Papaefstathiou and M. Spannowsky, arXiv:1404.7139 [hep-ph].
- [17] M. McCullough, arXiv:1312.3322 [hep-ph].
- [18] S. L. Hu, N. Liu, J. Ren and L. Wu, arXiv:1402.3050 [hep-ph].
- [19] The ATLAS collaboration, ATLAS-CONF-2013-060; The ATLAS collaboration, ATLAS-CONF-2013-056; S. Chatrchyan *et al.* [CMS Collaboration], Phys. Lett. B **729**, 149 (2014) [arXiv:1311.7667 [hep-ex]].
- [20] X. -F. Han, L. Wang, J. M. Yang and J. Zhu, Phys. Rev. D **87**, 055004 (2013) [arXiv:1301.0090];
- [21] L. Wang, J. M. Yang and J. Zhu, Phys. Rev. D **88** (2013) 075018 [arXiv:1307.7780 [hep-ph]].
- [22] J. Cao, F. Ding, C. Han, J. M. Yang and J. Zhu, JHEP **1311**, 018 (2013) [arXiv:1309.4939 [hep-ph]].
- [23] A. Denner, J. Kublbeck, R. Mertig and M. Bohm, Z. Phys. C **56**, 261 (1992).
- [24] N. Liu, J. Ren, L. Wu, P. Wu and J. M. Yang, JHEP **1404**, 189 (2014) [arXiv:1311.6971 [hep-ph]].
- [25] C. Englert and M. McCullough, JHEP **1307**, 168 (2013) [arXiv:1303.1526 [hep-ph]].
- [26] J. Beringer *et al.* [Particle Data Group Collaboration], Phys. Rev. D **86**, 010001 (2012).